Essential Readings in Light Metals: Aluminum Reduction Technology.
Edited by Geoff Bearne, Marc Dupuis and Gary Tarcy.

 From *Light Metals 1973*, A.V. Clack, Editor

COMPUTER MODEL FOR MAGNETIC FIELDS IN ELECTROLYTIC CELLS INCLUDING THE EFFECT OF STEEL PARTS

Th. Sele

Abstract

The computer model described in this paper calculates magnetic fields in electrolytic cells from an input of constructional data and known current distribution. Conventional formulas are used for the magnetic field from the current carrying system of the cell and its surroundings. A special method has been developed for the representation of steel parts in the model, in order to include their magnetic effect with reasonable accuracy. Principles are described and examples of calculations are given.

Th. Sele is electrical engineer at Årdal og Sunndal Verk, Sørkedalsveien 6, Oslo 3, Norway.

Introduction

The magnetic field program described in this paper is part of a larger model system developed by Årdal og Sunndal Verk (ÅSV), or by Institutt for Atomenergi on assignment from ÅSV, for the study of certain important properties of aluminium reduction cells. Other parts of the model system will also be presented at this AIME-meeting (1), (2) .

Magnetic fields together with electric currents create electromagnetic forces, and when such forces arise in the molten metal or the bath of the electrolytic cell they set up convection movements in the liquids and makes the metal surface convex and non-horizontal. The convection velocities are of interest because we believe they are largely responsible for the lowering of current efficiency. This paper will be limited to the description of the model for calculation of the magnetic field components, whereas turbulence velocities and curvature of the metal surface will be dealt with in the other system programs mentioned above.

Computer models for the calculation of magnetic fields in electrolytic cells have been developed by others, and have also been presented at earlier AIME meetings (3) . These models have however been limited to the calculation of magnetic fields arising from the current conductor system only, ignoring the effect of steel parts in the cell. The comparison of values calculated by these models and measured values may show relatively large deviations, because the effect of steel parts is appreciable.

It has been the aim for this magnetic model to include the effect of steel parts by an approximation method, so that the magnetic fields can be calculated from an input of constructional data for the cell and the potline, with a reasonable degree of accuracy in the results.

The model structure.

Reference axes and units.

All the elements which make up the model are referenced to a 3-dimensional axis system with its origo located in the center of the cell, on top of the carbon bottom as shown in fig. 1. The X-axis is always chosen in the same direction as the main potline current. The axes X-Y-Z follow each other in counterclockwise direction.

Lengths are given in meters, currents in kiloamps, and magnetic fields in gauss.

Model elements and their grading.

The magnetic fields are created by two principally different element types:

1. Current-carrying conductors.
2. Steel parts elements.

It is not satisfactory to limit the model to elements only for the pot under calculation,- current conductor elements on the neighbour pots and the whole surrounding potline are of high importance and cannot be neglected. In order to keep the model size and calculation work within reasonable limits it is necessary however to make a strong grading of details in the element representation, depending on the distance to the point under calculation. The grading is done as follows with reference to fig. 2.

Steel parts elements are included only for the pot under calculation, because their field contribution decreases with the square of the distance.

Input is given for a detailed model of current carrying conductors on the pot under calculation, with special care for details for the conductors close to the metal pad.

An extra set of input values is given for the representation of a simplified model version of the current system of a pot, the main busbars being represented as for the main model, but with all details substituted by a few simple conductors. The program manipulates with axis displacement on this simplified model to let it represent the surrounding neighbouring pots. As shown in fig. 2 there will be 5 neighbouring pots for a cell in the outer row, or 8 for a cell in the inner row.

The influence of current conductors in the potline further apart than the neighbour pots, is simplified in the model to consist of a single conductor running 100 meters in each direction with full potline current. This part of the model is generated by the program itself when the dimensions A, B and C in fig. 2 are given as input.

The potline configuration with 4 rows as shown in fig.2 is used in almost all ÅSV plants, and is chosen as standard for the model program. A configuration with 2 rows may however easily be calculated by specifying a very large value for the distance C. It should further be noted that positive values are specified for the distances B and C for a current direction as shown on fig. 2. With opposite current direction B and C are given negativ values in order to obtain correct field sign.

Current carrying elements.

As a principle all the current carrying parts in the cell and the potline are substituted in the model by cylindrical straight conductor elements running in the direction of one of the 3 main axes X, Y or Z.

Almost all the conductors in the real system are oriented in directions parallel to the main axis, so this is a most natural limitation which greatly simplifies input volume and calculation work. The formulas for obtaining the magnetic field components from such a conductor are shown in fig. 3.

For the representation of conductors outside the pot cavity, as for instance the large busbars alongside the cell, the radius of the current element is of no importance (and is normally specified as 0.1 m). For conductors located so that the point under calculation can be inside the conductor radius, this dimension must be fixed with great care because the field strength at the element surface is reduced linearly to zero in the center as indicated in fig.3. This is especially important for the elements representing the current path vertically through the anode, bath, and metal pad down to the cathode bars. This part of the model is also made up of cylindrical conductors of varying diameter filling the actual cross section with a slight overlap.

The whole current carrying system is substituted by such elements in the model, with strong grading of details as described in the previous chapter. When the magnetic field components shall be calculated at a certain point, the program collects the field contribution from each model element by using principally the same formula every time. This is a method well suited to computer work.

Steel parts element.

The steel constructions on electrolytic cells usually consist of a wide variety of complicated shapes. When trying to represent these parts in a model, two main points must be considered:

1. The real steel construction must be simplified in the model in order to keep the model volume and the calculation work within reasonable limits.
2. The model elements must be of such shape that they can be treated matematically by reasonable means.

As for point 1. It should be kept in mind that we are not interested in the magnetic flux within the steel parts as such, but only in the flux leaving these parts and penetrating into the cell cavity. In most cases there is a considerable distance between the more complicated steel parts and the metal pad in the cell. These facts permit a high degree of model simplification.

The problem according to point 2. consist in the determination of the so called "demagnetizing factor N" for a steel part of definite geometrical shape. This factor is matematically well defined for parts with the shape of an ellipsoid of revolution, and may be used with a reasonable degree of accuracy for cylindrical shapes with rounded ends.

According to above, the steel parts are substituted in the model by elements consisting of cylindrical rods with rounded ends, as magnetic dipoles, and there is made the further limitation that these dipoles must have a direction according to one of the 3 main axes. The dipole shall have the same length and cross section as the steel part it represents.

This principle is simple enough when applied to single rods and beams which may be substituted by single dipoles. For the representation of more complicated continous steel shapes, the principle must be extended to a system where the dipoles are linked together in the pole points. A very simple case is shown in fig. 5, where a steel anode stud is substituted by 3 dipoles.
When steel parts model is to be specified for a more complex structure, as for instance the bottom shell, many different solutions are possible, and a good deal of good judgement is required. In such cases it is advisable to start by considering the main magnetic flux distribution within the structure as shown on fig. 6. A continous flux in clockwise direction is produced in the upper part of the shell, because it is linked with the total pot current coming down from the anode to the cathode bars. The current now passes along the cathode bars out through the holes in the long sides of the shell, and thereby creates a magnetic flux in the opposite direction in the structure below these holes.In the short sides there is no such reverse of flux direction, as will be seen from fig. 6. With this flux picture in mind it is natural to design a dipole model as shown in fig. 7, with one upper ring of dipoles to take the upper flux, and another ring of dipoles for the structure below the cathode bar outlets, for the lower flux, and vertical dipoles connecting the two rings according to cross sections in the real structure. It is not necessary to insert a number of vertical dipoles corresponding to the number of outlets in the side, a much coarser model is normally satisfactory with a lumping together of cross sections for the dipoles.

A part of the bottom plate cross section should be included in the lower dipole ring, in order to take care of the flux which is added from these parts.

In fig. 7 is shown the flux direction in the dipole model as calculated by the program, and it is interesting to notice the correspondance with flux flow indicated in fig. 6. Fig.7 further has a + or - sign written on each pole point, indicating that flux is flowing out from or into the structure at these points. The numerical value is not shown for each point but one should notice how + and - poles are obtained in the 4 corners of the shell, especially concentrated at the upper part of the corners. The effect of this bottom shell magnetization on the total field picture will be shown in later examples.

<u>The principles for dipole magnetization</u> which are used in this program, are shown in fig. 4. The calculation must be done by an iteration method, because the magnetization of each single dipole depends upon:

a) Magnetizing field from current system.
b) Magnetizing field from the other dipoles.
c) Unlinear saturation characteristic.
d) Geometric shape (Demagnetizing factor N).

The field from the current conductor system is taken from the model. Magnetizing field from the other dipoles is taken from the steel parts model and is brought up to a final value through the iterative procedure. A common saturation characteristic for mild steel with saturation at 20 000 gauss is used for all steel parts. The demagnetizing factor N is calculated for each dipole according to its geometrical shape (L/D). When the field strength H is known in Oersted, the magnetization B for the dipole is determined according to the saturation curve and demagnetizing factor as shown in fig. 4.

A special problem is to define what is the real magnetizing field strength H for a dipole, when it is normally situated in an inhomogenous field. An average of many calculated values along the dipole might be used, but is rather time-consuming. It is chosen here to use the average of two values calculated for two points located at a certain distance "DIST" from the pole points, where the value of "DIST" is calculated from a formula as shown in fig. 4. The strongest and most inhomogehous part of exiting field for a dipole is that from its neighbour dipole linked to its pole point. The value of "DIST" is determined as a point where the demagnetizing effect from the pole points correspond to the demagnetizing factor. The formula is an approximation which holds well for long dipoles, and for the shorter ones the exact position is not of the same importance.

The finally calculated magnetic induction B for each dipole is not well suited to characterize the dipole effect outwards. A better value is the "pole strength" which is the field strength in gauss obtained from one pole point at a distance of 1 meter, and this value is used in the program.

Model input values and volume.

Each current system element is inserted in the model by one card, and a card for the element in fig. 3 would read as follows:

Z1 Z2 X Y RAD KAMP LETTER NO

The first 4 figures are the coordinates according to the figure, RAD is the radius and KAMP the current in kiloamps. LETTER and NO are a group letter and a number within the group, for identification where the data belong in the model.

Each magnetic dipole is inserted in the model accordingly by one card, and for a dipole in X-direction this would be as follows:

X1 X2 Y Z RAD POL LETTER NO

Here the first 4 figures are the coordinates in the same way as for the current element, and RAD is the dipole radius. POL is the "pole strength" of the dipole as defined in the preceding chapter, and the value is left open on the cards (=0) when they are read the first time because the values are not yet known. When the iterative calculation has been performed, the calculated values for POL are inserted on the cards, where they play an analogous role for the dipoles as the current does for the current elements. For calculating other versions in the model the POL-value on the cards serve as a starting value for the iterations.

The 3 dimensions A. B and C for potline geometry as shown in fig. 2 are given on one single input card together with total potline current and information whether calculation is wanted for a cell in inner or outer row.

The input volume for a calculation may vary considerably, but some characteristic figures might be some 250 cards for current system and 150 cards for steel dipoles.

Results from calculations.

The calculated values of magnetic field components in a network of points is always written out in tables. It is also possible to take out ready-made plots of "iso-gauss"-diagrams based on the calculated point-values. Such diagrams are shown in fig. 8 for the 3 resulting components for a 150 kA prebake pot, the section of which is shown in fig. 1.

It can be noted from fig. 8 c) that the vertical Z-component along the X-axis is about + 30 gauss although the cell has a symmetrical bus system. This is the effect of the current in the neighbour row, the spacing between rows being fairly close in this case.

It may be of interest to investigate a bit closer the effect of the steel parts in this picture, both in value and in shape. As an example we subdivide the Y-component in fig. 8 b) and show in fig. 9 how it is composed of a) Y-component from current system, b) Y-component from bottom shell, and c) Y-component from anode studs. It is interesting to notice how the bottom shell has a reducing (shielding) effect on the Y-component, of considerable magnitude. The effect from the anode studs is much smaller but somewhat more complex.

Comparison between measured and calculated values of magnetic field has been performed for some different cell types. A special measuring equipment has been developed and measurements are made in the metal pad under normal operating condition (4). The measuring points are usually located in two rows, one along each of the long sides of the anode, about 25 cm in from the side. The measurements may show great variations from pot to pot and from time to time, and average values for several pots are used for the comparison with calculated values. Devations between the measured and calculated values vary considerably and are usually largest towards the ends of the pot as might be expected. Deviations may well reach 30-35 % of the total field vector at single points, but as an average for the whole anode area the agreement is much better. In any case the deviations between measured and calculated values are much smaller with steel parts included in the model, than they were with the current system model only.

It may appear disappointing that the agreement is not better than this, but one should keep in mind that there are great limitations in the accuracy of the measurements even if the measuring equipment is fully reliable. Perhaps the most important source of inaccuracy is the positioning of the measuring probe. Even small displacements may result in quite strong field changes as will be evident from the diagrams in fig. 8. Other factors of importance are current variations, uneven current distribution and varying height of anode studs during measurements, resulting in considerable variations from pot to pot, and a relativ poor reproducibility.

As a conclusion we regard the calculated values from the magnetic model as giving a good picture of the magnetic condition of a cell, and we use the program extensively for the study of old and new pots. The model program enables us to use both current conductors and steel parts as active construction elements for the improvement of magnetic properties of the cells.

Acknowledgement.

The author is grateful to Årdal og Sunndal Verk for the permission to publish this work.

References.

1. Ek, A and Fladmark, G.E., "Simulation of Thermal, Electrical and Chemical Behaviour of an Aluminium Reduction Cell on a Digital Computer". 1973 AIME Meeting-Chicago.

2. Mueller, T.B. and Solberg, K.O., "Numerical Calculation of Mass Convection Patterns in an Aluminium Reduction Cell". 1973 AIME Meeting-Chicago.

3. Iuchi, T, "Rise and Flow of Molten Metal in Aluminium Reduction Cells". 1970 AIME Meeting - Denver.

4. Nebell, H. Internal ÅSV Reports.

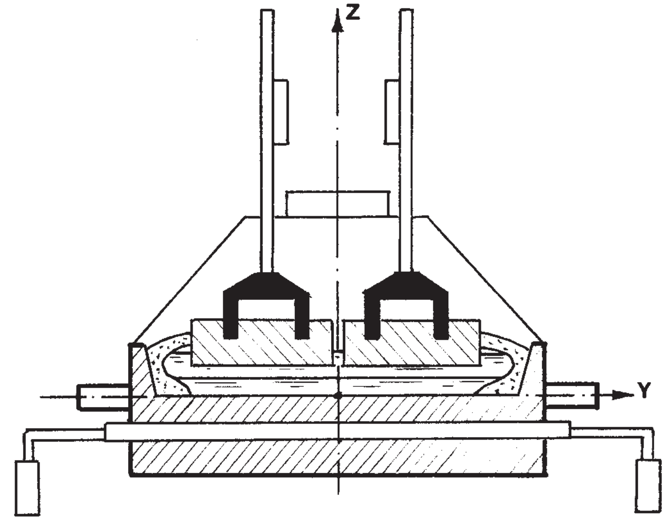

Fig.1 – Section of 150 kA cell

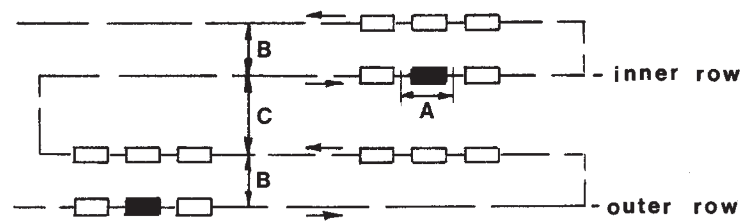

Fig.2 – Pot line geometry

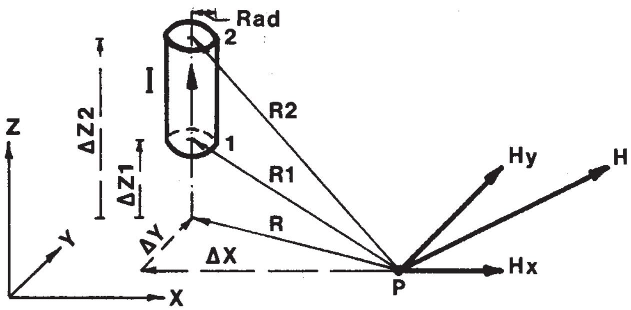

$$H_x = \frac{\Delta Y}{R} \cdot H = \frac{\Delta Y \cdot I}{R^2}\left(\frac{\Delta Z2}{R2} - \frac{\Delta Z1}{R1}\right)$$

$$H_y = -\frac{\Delta X}{R} \cdot H = -\frac{\Delta X \cdot I}{R^2}\left(\frac{\Delta Z2}{R2} - \frac{\Delta Z1}{R1}\right)$$

If $R < Rad$: $H = \frac{R}{Rad} \cdot H_{Rad}$

Fig. 3 – Magnetic field at P from current conductor 1–2

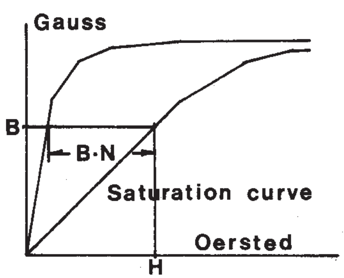

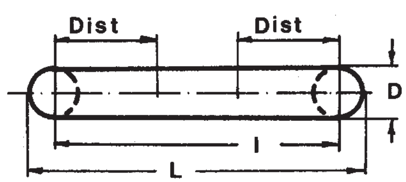

$$Dist \sim \frac{D}{4 \cdot \sqrt{N}}$$

Demagnetizing factor N (for rot. ellipsoid)

L/D	500	50	10	4	2	1	0
N	0.000024	0.0014	0.020	0.075	0.170	0.333	1.000

Fig. 4 – Principle of magnetic dipole

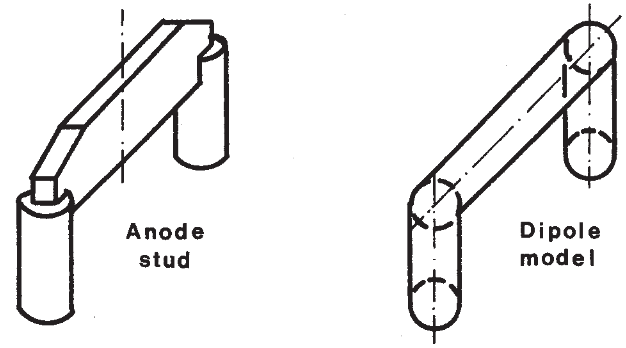

Fig. 5 – Dipole model of anode stud

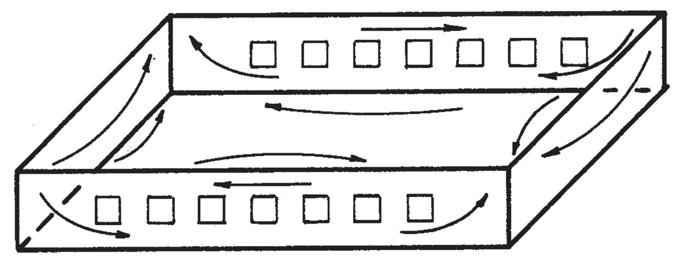

Fig. 6 – Main magnetic flux in bottom shell

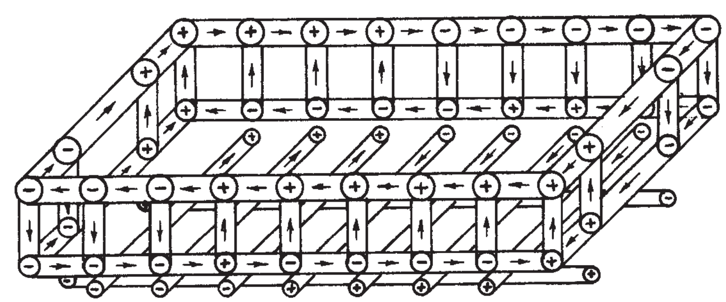

Fig. 7 – Dipole model of bottom shell and support beams

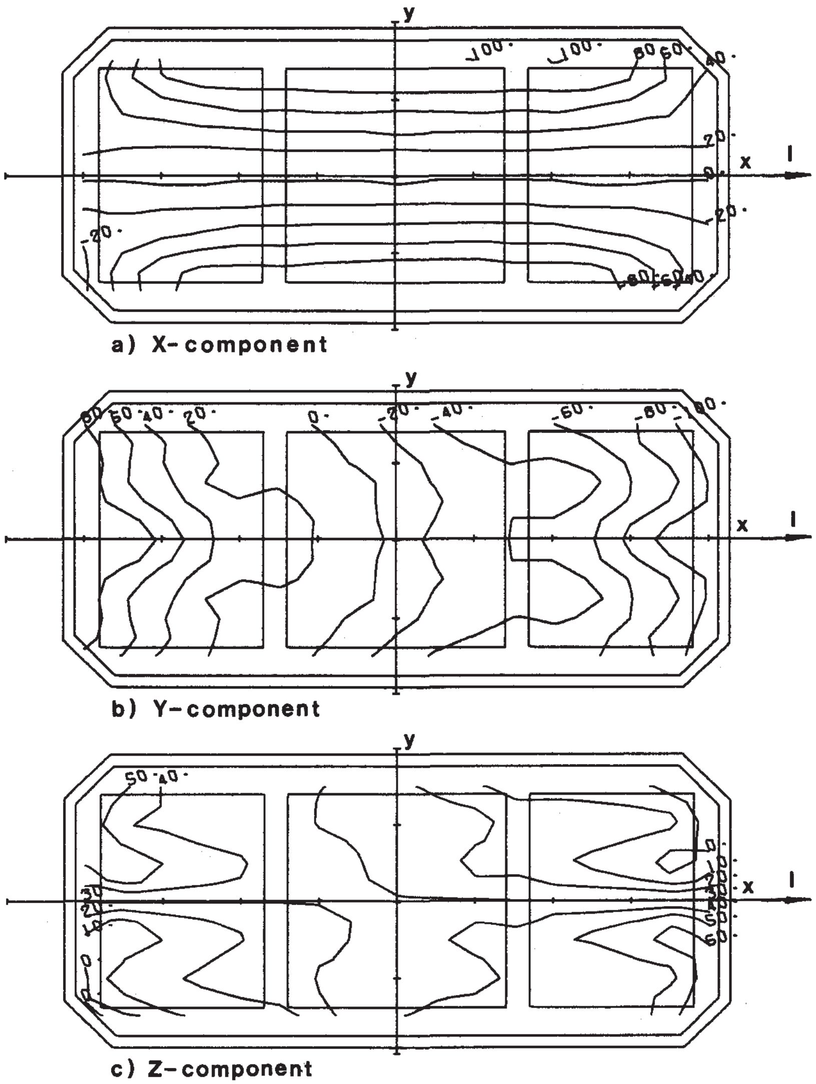

Fig.8– Magnetic field in 150 kA cell, in gauss. Height level Z=0.1 m.

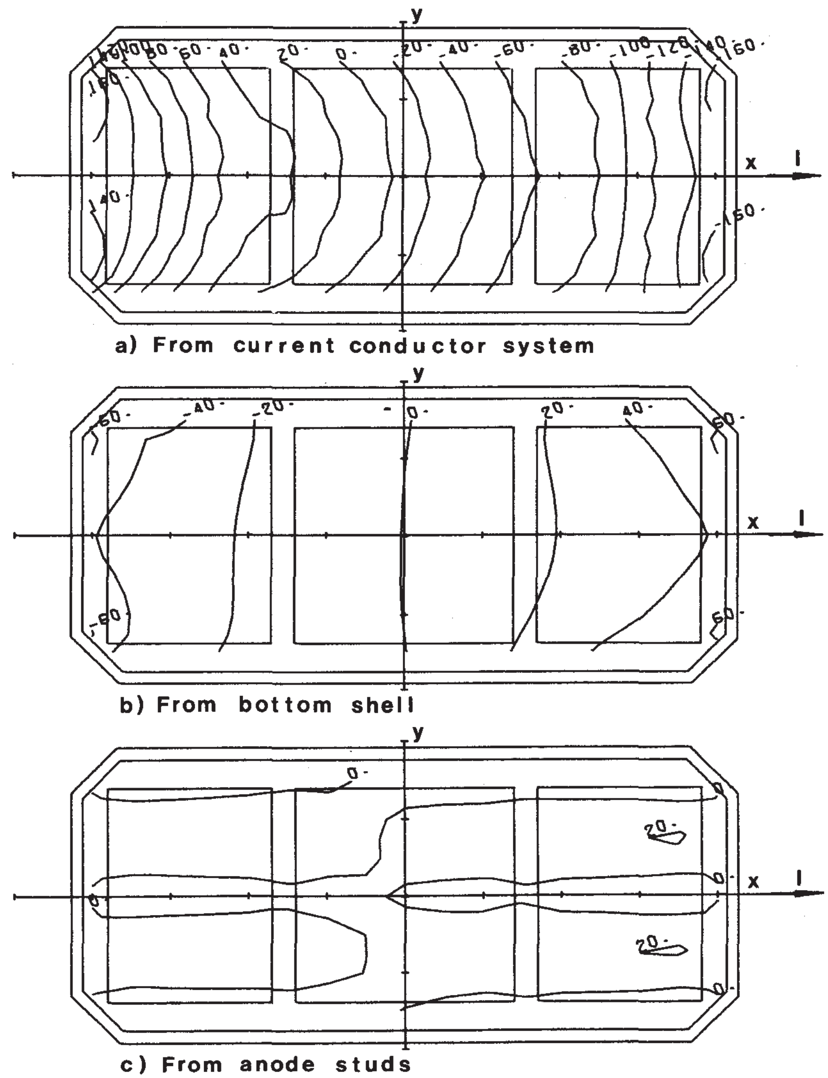

Fig.9 – Parts of Y-component in fig.8b